

Comprehensive evaluation of fluroxypyr herbicide on physiological parameters of spring hybrid millet

Meijun Guo¹, Jie Shen¹, Xi-e Song¹, Shuqi Dong¹, Yinyuan Wen¹, Xiangyang Yuan^{Corresp., 1}, Pingyi Guo^{Corresp. 1}

¹ Agronomy College, Shanxi Agricultural University, Taigu, China

Corresponding Authors: Xiangyang Yuan, Pingyi Guo

Email address: yuanxiangyang200@163.com, pyguo126@126.com

Foxtail millet (*Setaria italic* L.) is an important food and fodder crop that is cultivated worldwide. Quantifying the effects of herbicides on foxtail millet is critical for safe herbicide application. In this study, we analyzed the effects of different fluroxypyr dosages on the growth parameters and physiological parametric of foxtail millet, that is, peroxidation characteristics, photosynthetic characteristics, and endogenous hormone production, by using multivariate statistical analysis. Indicators were screened via Fisher discriminant analysis, and the growth parameters, peroxidation characteristics, photosynthesis characteristics and endogenous hormones of foxtail millet at different fluroxypyr dosages were comprehensive evaluated by principal component analysis. On the basis of the results of principal component analysis, the cumulative contribution rate of the first two principal component factors was 93.72%. The first principal component, which explained 59.23% of total variance, was selected to represent the photosynthetic characteristics and endogenous hormones of foxtail millet. The second principal component, which explained 34.49% of total variance, represented the growth parameters of foxtail millet. According to the principal component analysis, the indexes were simplified into comprehensive index Z, and the mathematical model of comprehensive index Z was set as $F = 0.592Z_1 + 0.345Z_2$. The results showed that the comprehensive evaluation score of fluroxypyr at moderate concentrations was higher than at high concentrations.

Consequently, 1 L (active ingredient, ai) ha⁻¹ fluroxypyr exerted minimal effects on growth parameters, oxidase activity, photosynthetic activity, and endogenous hormones, and had highest value of comprehensive evaluation, which had efficient and safe benefits in foxtail millet field.

Comprehensive evaluation of fluroxypyr herbicide on physiological parameters of spring hybrid millet

Meijun Guo¹⁺, Jie Shen¹, Xi-e Song¹, Shuqi Dong¹, Yinyuan Wen¹, Xiangyang Yuan^{1*}, and Pingyi Guo^{1*}

¹Agronomy College, Shanxi Agricultural University, Taigu, China

Author for correspondence: Pingyi Guo (E-mail: pyguo126@126.com)

Xiangyang Yuan (E-mail: yuanxiangyang200@163.com)

ABSTRACT

Foxtail millet (*Setaria italic* L.) is an important food and fodder crop that is cultivated worldwide. Quantifying the effects of herbicides on foxtail millet is critical for safe herbicide application. In this study, we analyzed the effects of different fluroxypyr dosages on the growth parameters and physiological parametric of foxtail millet, that is, peroxidation characteristics, photosynthetic characteristics, and endogenous hormone production, by using multivariate statistical analysis. Indicators were screened via Fisher discriminant analysis, and the growth parameters, peroxidation characteristics, photosynthesis characteristics and endogenous hormones of foxtail millet at different fluroxypyr dosages were comprehensive evaluated by principal component analysis. On the basis of the results of principal component analysis, the cumulative contribution rate of the first two principal component factors was 93.72%. The first principal component, which explained 59.23% of total variance, was selected to represent the photosynthetic characteristics and endogenous hormones of foxtail millet. The second principal component, which explained 34.49% of total variance, represented the growth parameters of foxtail millet. According to the principal component analysis, the indexes were simplified into comprehensive index Z, and the mathematical model of comprehensive index Z was set as $F = 0.592Z_1 + 0.345Z_2$. The results showed that the comprehensive evaluation score of fluroxypyr at moderate

concentrations was higher than at high concentrations. Consequently, 1 L (active ingredient, ai) ha⁻¹ fluroxypyr exerted minimal effects on growth parameters, oxidase activity, photosynthetic activity, and endogenous hormones, and had highest value of comprehensive evaluation, which had efficient and safe benefits in foxtail millet field.

INTRODUCTION

Foxtail millet (*Setaria italica* L.) is a valuable economic crop because it is rich in protein and crude fat and used as a staple food worldwide. This plant has seven essential amino acids, and its contents are higher than those found in other crops. In particular, methionine and tryptophan, which are important in preventing atherosclerosis and softening the blood vessel, are abundant in this plant. However, weed infestation has severely limited foxtail millet production in China (Guo et al., 2018). Weeds are the most important biotic factor affecting agricultural production; they are responsible for over 55.56% of total foxtail millet yield losses (Zhou et al., 2012). For weed control, herbicide application is considered the most cost-efficient and effective method (Rubin, 1996). Rational application of herbicides, such as monosulfuron, monosulfuron mix propazine, 2,4-D, and prometryn, can effectively control weeds in foxtail millet fields; however, these herbicides readily cause phytotoxicity reaction (Tian & Wang, 2010). Thus, finding suitable herbicides for use in foxtail millet field is a considerable challenge in weed control.

Fluroxypyr (4-amino-3, 5-dichloro-6-fluoro-2-pyridyloxyacetic acid) is originally applied in cereal, olive tree, and fallow cropland fields, to control annual or perennial weeds (Hellou et al., 2009). These herbicides cause auxin overdose or excessive endogenous auxin concentrations, thereby resulting in an imbalance of auxin homeostasis and interaction with other hormones in tissues, which ultimately cause the succeeding series of biochemical and physiological processes associated with herbicide action (Grossmann, 2010). Liu (2014)

demonstrated that the label fluroxypyr dose can be used in maize (*Zea mays*) and winter wheat (*Triticum aestivum*) fields, and has desirable control effects on broadleaf weeds. Considering the significant differences in the sensitivity of crop varieties to fluroxypyr, it is necessary to indicate whether fluroxypyr is safe for use on foxtail millet.

Foxtail millet tolerance toward herbicides depends on either the alteration of the target site (TS) or non-target site (NTS) mechanisms. TS resistance mechanism is manifested by structural changes due to point mutations in herbicide-binding proteins, such as the D1 protein in the photosystem II (PSII) complex (Thiel & Varrelmann, 2014), acetolactate synthase (Tranel, Wright & Heap, 2014), acetyl-CoA carboxylase (Kaundun, 2014), or 5-enolpyruvylshikimate-3-phosphate synthase (EPSPS) (Sammons & Gaines, 2014). TS resistance mechanism is occasionally the result of an increased number of copies of the target gene, such as EPSPS (Gaines et al., 2010; Vila-Aiub et al., 2014). The NTS mechanism involves herbicide detoxification by glutathione S-transferase or cytochrome P450 monooxygenase, reduced absorption or translocation in the plant and sequestration into vacuoles (Matzrafi et al., 2014). In contrast to TS, NTS resistance mechanisms can occasionally be more widespread and exhibit resistance to many herbicides. However, information regarding the physiological mechanism of Zhangzagu hybrid millet after the application of fluroxypyr is limited. Thus, the NTS resistance mechanisms to fluroxypyr in spring hybrid millet should be understood.

The hybrid foxtail millet ‘Zhangzagu’ is popular, especially Zhangza 5, with a large production area in China due to its high yield, drought resistance, and nutritional value (Dong et al., 2014). Thus, we used Zhangza 5 as the model species for the present study, especially for the study of the physiological mechanism due to tolerance against fluroxypyr. Herein, the objective of this study are as follows: (1) to comprehensively investigate the influence of different dosages of fluroxypyr on the growth and physiological mechanism of

spring hybrid millet; (2) to further understand the NTS resistance mechanisms to fluroxypyr-induced oxidative stresses; (3) to compare and analyze the main factors contributing to the effect of fluroxypyr on spring hybrid millet growth. Thus, we provided convincing evidence for the correlations of NTS resistance to fluroxypyr exposure, and aimed at obtaining the optimal fluroxypyr application dose for spring hybrid millet.

MATERIALS AND METHODS

Plant and experimental design

Fluroxypyr (20%, emulsifiable concentrate) was provided by Dow AgroScience Co. (Jiangsu, China). Foxtail millet (*Setaria italica* L. cv. Zhangza 5) was supplied by the Zhangjiakou Academy of Agricultural Sciences of Hebei Province, China. The seeds were uniformly sown in a plastic pot (130 mm diameter) containing a mixture of sand and soil (1:2, v:v). Calcareous cinnamon soil, with a pH of 7.85, 24.49 g kg⁻¹ organic matter, 51.92 mg kg⁻¹ total nitrogen, 24.13 mg kg⁻¹ available phosphorus, and 183.6 mg kg⁻¹ rapidly-available potassium was used in this work. At the three-leaf stage, the foxtail millet seedlings were thinned and maintained at 10 uniform plants per pot.

The experiment was conducted as a randomized complete block design with three replications. After growing to the five-leaf stage, foxtail millet seedlings were treated with 0, 0.5, 1, 2, and 4 L ai ha⁻¹ fluroxypyr by using a laboratory pot-sprayer equipped with a nozzle and previously calibrated to deliver 450 L ha⁻¹. The manufacturer recommended an effective dose of 1 L ai ha⁻¹ for field application. After herbicide treatment for 5 and 10 days, the physiological indices of all foxtail millet seedlings were analyzed.

Measurement of growth parameters

The plant height, length and width of leaves were measured with a ruler. Leaf area was calculated using the following equation: leaf area = 0.75 × leaf length × leaf width. Leaf width was considered the widest part of

the penultimate leaf.

Determination of superoxide generation rate and H₂O₂ content

Fresh foxtail millet leaves (0.1 g) were homogenized with 2 mL of 65 mmol L⁻¹ sodium phosphate buffer (pH 7.8) and centrifuged at 10,000 rpm for 10 min. The supernatant (1 mL) was mixed with 1 mL of 65 mmol L⁻¹ sodium phosphate buffer (pH 7.8) and 0.2 mL of 10 mmol L⁻¹ hydroxyl ammonium chloride. The resulting supernatant was incubated 25°C for 20 min, and the above reaction mixture (1 mL) was mixed with 1 ml of 4-aminobenzene sulfonic acid (17 mmol L⁻¹) and 1 mL of α -naphthylamine (7 mmol L⁻¹), then incubated at 30 °C for 30 min. The absorbance at 530 nm was measured with a 756C-UV-VIS spectrophotometer (Shanghai Spectrum Instruments Co. Ltd) (Elstner & Heupel, 1976).

Fresh foxtail millet leaves (0.1g) were homogenized with 5 mL of chilled acetone in an ice bath and centrifuged at 4,000 rpm for 15 min. The supernatant (1 mL) was mixed with 0.1 mL of 20% TiCl₄ concentrated hydrochloric acid and 0.2 mL of concentrated ammonium hydroxide. The reaction mixture was centrifuged at 10,000 rpm for 10 min and the precipitate was dissolved in 3 mL H₂SO₄ (1 mol L⁻¹). The absorbance of the supernatant at 410 nm was monitored with a 756C-UV-VIS spectrophotometer (Zhang et al., 2012).

Determination of antioxidant enzyme activities

Fresh foxtail millet leaves (0.1g) were homogenized with 2 mL of sodium phosphate buffer (pH 7.0, containing 0.1 mmol L⁻¹ EDTA and 1% PVP (w/v)) in an ice bath. The homogenate was centrifuged at 10,000 rpm for 15 min at 4°C. The supernatant was extracted and used to measure the activities of superoxide (SOD), peroxidase (POD), catalase (CAT), and ascorbate peroxidase (APX). The samples were measured with a 756C-UV-VIS spectrophotometer.

SOD activity was analyzed by using the nitro blue tetrazolium (NBT) method. The reaction mixture (5 mL) consisted of phosphate buffer (50 mmol L⁻¹, pH 7.8), L-methionine (13 mmol L⁻¹), NBT (0.075 mmol L⁻¹), EDTA (0.1 mmol L⁻¹), riboflavin (0.002 mmol L⁻¹), and 20 µL of enzyme extract. The reaction mixture was then illuminated under 4000 lx for 15 min at 25°C. One unit of activity corresponds to the amount of protein required to inhibit 50% of the initial reduction of NBT under light conditions. The absorbance at 560 nm was measured, and a non-irradiated complete reaction mixture served as the control. For POD activity determination, 20 µL of enzyme extract was added into 3 mL of reaction liquid containing 3 mL of sodium phosphate buffer (100 mmol L⁻¹, pH 6.0), 19 µL of guaiacol, and 28 µL of 30% H₂O₂. POD activity was measured by the changes in the absorbance of the reaction solution at 470 nm for 3 min. For CAT activity determination, the reaction liquid consisted of 2.7 mL of Tris-HCl (50 mmol L⁻¹, pH 7.0), 50 µL of H₂O₂ (200 mmol L⁻¹), and 20 µL of enzyme extract. Enzyme activity was continuously determined at 240 nm for 3 min following H₂O₂ decomposition. In accordance with the method of APX activity determination by Nakano & Asada (1981), the reaction mixture consisted of 3 mL sodium phosphate buffer (50 mmol L⁻¹, pH 7.0), 0.4 mL of EDTA (0.3 mmol L⁻¹), 1 mL of ascorbate (0.9 mmol L⁻¹), and 1 mL of enzyme extract. The reaction mixture was then incubated for 5 min at 25 °C. The above reaction mixture was mixed with 0.5 mL of H₂O₂ (0.25 mmol L⁻¹), and H₂O₂ decomposition was measured by the decline in absorbance at 290 nm for 1 min.

Glutathione reductase (GR) activity was analyzed according to Halliwell & Foyer (1978). Fresh foxtail millet leaves (0.1g) were ground in an ice bath with 2 mL of Tris-HCl (pH 7.5, containing 1% PVP and 0.1 mmol L⁻¹ EDTA), and centrifuged at 10,000 rpm for 15 min at 4°C. The enzyme extract (150 µL) was added into 3 mL of reaction liquid including Tris-HCl (pH 7.5), MgCl₂ (3 mmol L⁻¹), GSSG (0.5 mmol L⁻¹), and NADPH (0.15 mmol L⁻¹). Enzyme activity was calculated by the change in absorbance at 340 nm for 3 min.

Determination of photosynthetic gas exchange and chlorophyll

Photosynthetic rate (P_N), transpiration rate (E), and stomatal conductance (G_s) were measured by CI-340 portable photosynthesis system (CID Bio-Science, Inc., USA) from 9:30 to 10:30 am. The photosynthetically active radiation (PAR) at the leaf surface was approximately $11000 \pm 50 \mu\text{mol}/\text{m}^2/\text{s}$, the temperature of the leaf chamber was $30 \pm 2 \text{ }^\circ\text{C}$, and the ambient CO_2 concentration was $380 \pm 50 \mu\text{mol}/\text{mol}$.

To measure photosynthetic pigments, fresh leaves (0.1g) were soaked in 10 mL of ethanol (96%, v/v) and stored in the dark for 24 h. The absorbance of the supernatants was measured at 649 and 665 nm with a 756C-UV-VIS spectrophotometer (Lichtenthaler, 1987).

Measurement of chlorophyll fluorescence and P_{700} parameters

The chlorophyll fluorescence and P_{700} parameters were simultaneously detected using a luminoscope (Dual PAM-100, WALZ, Germany) (Pfündel, Klughammer & Schreiber, 2008). After dark adaptation for 30 minutes, the kinetics of chlorophyll fluorescence induction and P_{700} oxidation were simultaneously detected according to the “Fluo + P_{700} ” analysis mode.

First, the minimal fluorescence (F_0) was detected under weak light ($7 \mu\text{mol}/\text{m}^2/\text{s}$). Subsequently, the maximum fluorescence (F_m) was determined by the saturation pulse ($4000 \mu\text{mol}/\text{m}^2/\text{s}$, 800 ms) method. The slow induction curve was calculated as follows: $F_v/F_m = (F_m - F_0)/F_m$, $\text{ETR}_{\text{II}} = \text{PAR} \times 0.84 \times 0.5 \times Y_{\text{II}}$, $Y_{\text{II}} = (F_m' - F)/F_m'$, $Y_{\text{NO}} = 1/(\text{NPQ} + 1 + q_L (F_m/F_0 - 1))$, $Y_{\text{NPQ}} = 1 - Y_{\text{II}} - Y_{\text{NO}}$, where F_v/F_m and Y_{II} are the maximum PSII quantum yield and effective PSII quantum yield, respectively, and Y_{NPQ} and Y_{NO} are the regulated energy dissipation and non-regulated energy dissipation, respectively.

P_{700} oxidation was monitored by the changes in the transmittance signals at 875 nm and 830 nm (Klughammer & Schreiber, 2008). The maximal P_{700} (P_m) was denoted by the maximal P_{700} signal reduction to

full oxidation. Y_{NA} , the nonphotochemical quantum yield of PSI, is a measure of the acceptor-side limitation and calculated according to the formula $Y_{NA} = (P_m' - P_m)/P_m'$. Y_I , the photochemical quantum yield of PSI, was calculated according to the formula $Y_I = (P_m' - P)/P_m$. Y_{ND} , the nonphotochemical quantum yield of PSI, is a measure of the donor side limitation and calculated as $Y_{ND} = (P - P_0)/P_m$. The sum of these three quantum yields is one, i.e.: $Y_I + Y_{ND} + Y_{NA} = 1$. The electron transfer efficiency of PSI, ETR_I was assessed by the Dual PAM software.

Measurement of endogenous hormones

Fresh foxtail millet leaves (0.5 g) were homogenized with 4 mL of 80% methanol (1 mmol/L 2, 6-di-tert-butyl-4-methylphenol) in an ice bath. The homogenate mixture was refrigerated at 4 °C for 4 h, and centrifuged at 3,500 rpm for 8 min. The precipitate was added to 1 mL of 80% methanol, refrigerated at 4 °C for 1 h, and centrifuged. The supernatant passed through a C_{18} solid phase extraction column, and then dried with nitrogen. The hormone extract was obtained by mixing with 1 mL of the sample diluent (PBS containing 0.1% Tween-20, gelatin 1 µg/L) and determined using enzyme-linked immunosorbent assay. The hormone assay kit was supplied by China Agricultural University, and the content of auxin (IAA), abscisic acid (ABA), zeatin (ZR), and gibberellin (GA) contents were measured by using the Thermo Multiskan FC enzyme-labeled instrument.

Statistical analysis

Statistical analyses were performed using Statistical Product and Service Solutions 19.0 (SPSS Inc., Chicago, IL). Quantitative data were expressed as the mean \pm standard error, and multiple comparisons were analyzed by Duncan's multiple range test. $P < 0.05$ was considered significantly different. In this study, Fisher discriminant and principal component analyses (PCA) were calibrated by using the selected indices with the

highest difference between the different herbicide treatments and control, to simplify the indicators.

RESULTS

Effects of fluroxypyr on growth parameters

After exposing the seedlings to 0.5–4.0 L ai ha⁻¹ fluroxypyr for 5 days, the plant height of Zhangza 5 significantly differed between the control and herbicide treatments. At 10 days post-fluroxypyr treatment, the plant height increased by 10.16%, 12.62%, and 5.73% after exposure to 0.5, 1.0, and 2.0 L ai ha⁻¹, respectively. As shown in Table 1, the leaf area of Zhangza 5 significantly differed between the recommended dose (1 L ai ha⁻¹) and other treatments after 5 days. A similar response of the leaf area was recorded when Zhangza 5 was exposed to fluroxypyr for 10 days, thereby showing significant difference among treatments compared with the recommended dosage.

Effects of fluroxypyr on stress parameters

Fluroxypyr treatment at doses ranging from 0 to 4 L ai ha⁻¹ increased H₂O₂ and O₂⁻ accumulation in plants, with the maximum expression levels obtained after treatment with a dosage of 4 L ai ha⁻¹ for 5 and 10 days. As shown in Table 2, maximum H₂O₂ and O₂⁻ accumulations significantly increased by treatment with 4 L ai ha⁻¹ fluroxypyr for 5 and 10 days compared with the control. Similarly, treatment with fluroxypyr at the recommended dose (1 L ai ha⁻¹) increased H₂O₂ and O₂⁻ contents by 1.01- and 1.02- fold relative to the control after 5 days and by 2.02- and 1.05-fold relative to the control after 10 days, respectively. In our studies, we observed a time-dependent decrease in reactive oxygen species (ROS) in response to fluroxypyr exposure.

Effects of fluroxypyr on enzyme activities

As shown in Figure 1, the SOD, POD, CAT, APX, and GR activities significantly increased. The exposure of Zhangza 5 to increasing levels of fluroxypyr led to increases in SOD, CAT, APX, and GR

activities. However, further increases in fluroxypyr concentration beyond 2 L ai ha⁻¹ failed to promote SOD, CAT, APX, and GR accumulation. The activities of SOD, CAT, APX, and GR significantly increased after treatment with 2 L ai ha⁻¹ fluroxypyr relative to the control. POD activities were stimulated after exposure to different fluroxypyr concentrations, and its effect was concentration-dependent; the highest POD activity was observed at 4 L ai ha⁻¹ fluroxypyr. POD activities significantly increased by 2.91- and 3.53- fold relative to the control after treatment with 4 L ai ha⁻¹ fluroxypyr for 5 and 10 days, respectively.

Effects of fluroxypyr on net photosynthetic rate and pigments

As shown in Table 3, P_N , E , G_s , and Chl showed a progressive decrease with increasing fluroxypyr concentration. After 1 L ai ha⁻¹ (recommended dose) fluroxypyr treatment for 5 days, P_N and E significantly decreased by 23.72% and 22.56% compared with the control, respectively. However, 1 L ai ha⁻¹ fluroxypyr treatment for 5 days inhibited G_s by 3.53%. Moreover, after with 1 L ai ha⁻¹ fluroxypyr for 10 days, P_N , E , and G_s of the treated plants were reduced by 18.78%, 15.12%, and 18.79% compared with the control, respectively. According to our results, significant differences were recorded between the treatments and control. Chlorophyll content was also significantly affected following fluroxypyr treatment; however, no significant differences were observed between the control and treatment using the recommended dose after 5 and 10 days of exposure.

Effects of fluroxypyr on chlorophyll fluorescence and P_{700} parameters

After 5 days of exposure to fluroxypyr, the F_v/F_m of treated plants decreased to 0.13%, 0.32%, 1.71%, and 3.29% compared with the control, and the differences between treatments were insignificant. Moreover, after 10 days, the F_v/F_m of the treated plants recovered to control levels. As shown in Figure 2, the changes in $Y(II)$ and $ETR(II)$ were consistent under fluroxypyr treatment, and the values were reduced in a dose-dependent

manner. After 5 and 10 days of treatment, Y(II) decreased from 12.44% to 22.96%, and from 18.25% to 32.14%, respectively, and ETR(II) decreased from 12.37% to 22.69%, and from 14.91% to 32.31%, respectively. Additionally, Y(NPQ) increased with increasing fluroxypyr doses, and the maximum accumulation was observed at 2 L ai ha⁻¹. During treatment with 2 L ai ha⁻¹ fluroxypyr, the Y(NPQ) values were 36.39%, and 50.75%, compared with the control.

PSI activities were substantially affected by fluroxypyr treatment. As shown in Figure 2, Pm, Y(I), and ETR(I) were evidently decreased with increasing fluroxypyr dosage; however, no significant differences between the control and herbicide-treated plants were observed after 5 days of exposure. Treatment with increasing fluroxypyr concentration increased the Y(ND) of Zhangza 5. The maximum Y(ND) level was observed at fluroxypyr treatment. However, further increasing the dosages of fluroxypyr beyond 2 L ai ha⁻¹ no longer increased Y(ND).

Effects of fluroxypyr on endogenous hormones

Fluroxypyr treatment at doses ranging from 0.5 to 4 L ai ha⁻¹ increased IAA and ABA accumulation in plants, with the maximum accumulation observed at 4 L ai ha⁻¹ (Figure 3). The application of 4 L ai ha⁻¹ fluroxypyr significantly increased IAA and ABA by 26.69% and 23.36% relative to that of the control after 5 days of treatment and 5.37% and 35.53% relative to that of the control after 10 days of treatment, respectively. A similar response was observed between GA and ZR accumulation in Zhangza 5 exposure to fluroxypyr; GA and ZR decreased with increasing fluroxypyr concentration, and the difference observed between the control and treated plants was significant. After treatment with 1 L ai ha⁻¹ (recommended dose) fluroxypyr for 5 and 10 days, the GA and ZR values significantly decreased by 10.46%, 18.72%, and by 13.50%, 23.59% relatively to the control treatment, respectively.

Comprehensive evaluation of fluroxypyr on various foxtail millet indices

To further comprehensively evaluate the effects of fluroxypyr on various foxtail millet indices, Fisher discriminant analysis was used. Herbicide treatment was used as the grouping variable Y, and the physiological parameters were used as the independent variable X.

(1) Fisher discrimination was used to evaluate the seven indicators of foxtail millet leaf, namely, $H_2O_2(X_1)$, $O_2^- (X_2)$, $SOD(X_3)$, $POD(X_4)$, $CAT(X_5)$, $APX(X_6)$, and $GR(X_7)$. The following discriminant functions were obtained:

$$Y_1 = -3.850 + 4.868X_3 + 3.588X_6 - 48.734X_7$$

$$Y_2 = -0.344 - 1.408X_3 + 2.886X_6 - 7.736X_7$$

$$Y_3 = -5.062 - 0.107X_3 + 0.020X_6 + 12.487X_7$$

The cumulative contribution rate of the first-class functions, which is the main function, reached 98.8%. Thus, $SOD(X_3)$, $POD(X_4)$, and $GR(X_7)$ were used as indices to evaluate the peroxidation characteristics of foxtail millet.

(2) Fisher discrimination was used to evaluate the fourteen indicators of foxtail millet leaf, namely, $P_N(X_1)$, $E(X_2)$, $G_s(X_3)$, $Chl(X_4)$, $F_v/F_m(X_5)$, $Y(II)(X_6)$, $ETR(I)(X_7)$, $Y(NPQ)(X_8)$, $Y(NO)(X_9)$, $P_m(X_{10})$, $Y(I)(X_{11})$, $ETR(I)(X_{12})$, $Y(ND)(X_{13})$, and $Y(NA)(X_{14})$. The following discriminant functions were obtained:

$$Y_1 = -252.994 + 427.640X_6 - 66.364X_8 + 143.154X_{10} + 1.396X_{12}$$

$$Y_2 = -69.158 + 151.904X_6 + 96.548X_8 + 22.743X_{10} - 0.036X_{12}$$

$$Y_3 = -5.251 - 91.400X_6 - 1.385X_8 + 7.042X_{10} + 0.184X_{12}$$

$$Y_4 = 1.257 + 2.323X_6 - 1.378X_8 + 3.767X_{10} - 0.018X_{12}$$

The cumulative contribution rate of the first-class functions, which is the main function, reached 94.4%.

Thus, $Y(II)(X_6)$, $Y(NPQ)(X_8)$, $P_m(X_{10})$, and $ETR(I)(X_{12})$ were used as indices to evaluate the photosynthetic characteristics of foxtail millet.

(3) Fisher discrimination was used to evaluate the four indicators of foxtail millet leaf, namely, $IAA(X_1)$, $GA(X_2)$, $ZR(X_3)$, and $ABA(X_4)$. The following discriminant functions were obtained:

$$Y_1 = -78.315 + 8.217X_2 + 0.229X_4$$

$$Y_2 = -13.841 + 1.139X_2 + 0.073X_4$$

The cumulative contribution rate of the first-class functions, which is the main function, reached 94.4%. Thus, $GA(X_2)$ and $ABA(X_4)$ were used as indices to evaluate the endogenous hormone characteristics of foxtail millet.

As shown in Table 4, the cumulative contribution rate of the first two principal components reached 93.72%. Thus, the first two principal components were further analyzed. The first principal component accounted for 59.23% of the variance observed, whereas the second principal component accounted for 34.49% of this variance. The load values of $ERT(I)$, $Y(II)$, and GA , which were 0.978, 0.975 and 0.963, respectively, were the largest in the first principal component. ABA also showed high absolute loading value in the first principal component, but exhibited a negative effect. Therefore, the first principal component could explain the photosynthetic characteristics and endogenous hormones of foxtail millet. In the second principal component, the loading values of plant height and leaf area were relatively high and could represent the growth parameters of foxtail millet.

According to the principal component analysis, the model was set up as follows: $F = 0.592Z_1 + 0.345Z_2$. The comprehensive evaluation scores of the 2 and 4 L ai ha⁻¹ fluroxypyr treatments were relatively low, which indicated that high fluroxypyr concentrations negatively affected the photosynthetic characteristics and

endogenous hormones of foxtail millet. Furthermore, the comprehensive evaluation scores of the 0.5 and 1 L ai ha⁻¹ fluroxypyr treatments were 0.941 and 2.007, respectively, and the scores of first two principal components were positive, which indicated that the moderate concentrations of fluroxypyr positively affected the peroxidation characteristics, photosynthetic characteristics, and endogenous hormones of foxtail millet (Table 5). Consequently, the scores of the two factors in 1 L ai ha⁻¹ fluroxypyr treatments were both relatively high and represented the comprehensive effect of herbicide in foxtail millet (Figure 4).

DISCUSSION

Numerous studies have demonstrated that excessive application of fluroxypyr in the environment inhibits plant growth (Guo et al., 2010; Guo et al., 2018). In the present study, we found that fluroxypyr had a slight effect on plant growth at relatively low doses, but exerted significant influence at high doses. The growth inhibition of fluroxypyr is closely related to the accumulation of O₂⁻ and H₂O₂ in plants (Guo et al., 2010). According to the inhibitory effect of fluroxypyr on ROS, the present study showed that the maximum accumulation of H₂O₂ and O₂⁻ occurs when plants are treated with 4 L ai ha⁻¹ fluroxypyr for 5 and 10 days.

Herbicide-induced oxidative stress causes cellular peroxidation and molecular damage through ROS over-accumulation (Kehrer, 1993; Chen et al., 2009). To inhibit ROS action, plants have evolved protective enzymatic mechanisms, such as those involving SOD, POD and CAT (Khan & Kour, 2007). In most cases, the enzyme-based antioxidant system is one of the important ways for plants to resist environmental stress, which reflects not only the level of toxicity but also the ability to tolerate stress. Our analyses showed that the SOD, POD, CAT, APX, and GR activities generally increased at low fluroxypyr dosages but decreased at high fluroxypyr dosages, thereby reflecting an increased degree of oxidative stress.

Several symptoms related to changes in plant photosynthesis were observed in this work. After fluroxypyr

treatment, one such visible symptom was chlorosis, which showed that chlorophyll was certainly sensitive to fluroxypyr exposure. In the present study, chlorophyll formation was considerably suppressed at high concentrations (2 and 4 L ai ha⁻¹). A reduction in P_N , as reflected by the decrease in E and G_s , was also noted after fluroxypyr treatment. These results suggested that fluroxypyr destroyed the chloroplast structure of foxtail millet, increases the risk of photo-oxidation damage, and reduced light absorption, transmission, and distribution between PSII and PSI (Havaux, Strasser & Creppin, 1991).

Chlorophyll and gas exchange measurements are nondestructive methods used to identify the modes of action of certain herbicides in the ecological risk assessment of herbicide exposure. In this study, chlorophyll fluorescence showed that fluroxypyr treatment affected photosynthesis efficiency, even in the absence of phenotypic symptoms (Qian et al., 2014). Our analyses showed that each fluroxypyr treatment caused different degrees of F_v/F_m decrease, and the differences among treatments after 5 days of exposure were insignificant. Compared with the control, only the maximum fluroxypyr dose (4-fold the recommended dose) showed significantly reduced F_v/F_m values. Given that fluroxypyr inhibited electron transport in Zhangza 5, it also caused the decline in $Y(II)$ and $ETR(II)$. $Y(NPQ)$ represents the regulated photo-protective NPQ mechanism, namely, dissipating the fraction of energy in the form of heat (Christof & Ulrich, 2008). $Y(NPQ)$ also dissipates excess PSII energy via the xanthophyll cycle and associated carotenoids (Deng et al., 2013). In the present study, fluroxypyr treatment caused the increase in $Y(NO)$, which demonstrated that the plant cannot protect itself against damage from excess illumination due to blocking the regulatory mechanism of the non-photochemical dissipation of energy. Consistent with our results, Guo et al. (2018) reported that sethoxydim has similar effects on the photosynthetic pigments, photosynthetic gas exchange and chlorophyll fluorescence parameters of foxtail millet.

Previous studies on several plant species have demonstrated that a typical feature of PSI photoinhibition is the reduction in the maximum oxidation reduction ability of PSI (Scheller & Haldrup, 2005). In the present study, P_m , $Y(I)$, and $ETR(II)$ decreased with increasing fluroxypyr doses, and were significantly inhibited compared with those of the control. Fluroxypyr inhibited electron transport in Zhangza 5, which caused an increase in $Y(NA)$. $Y(NA)$ is an important photo-damage indicator in PSI, and it is affected by dark adaptation and level of damage to CO_2 fixation. $Y(NA)$ was significantly increased by treatment with $> 2 \text{ L ai ha}^{-1}$ fluroxypyr dose, showing that fluroxypyr aggravated the injury of PSII in foxtail millet leaves, reduced electronic accumulation of acceptor-side in PSI, blocked the dark reaction process, and decreased the fixed amount of CO_2 . $Y(ND)$ reflected the state of electron donors in PSI and is affected by the transmembrane proton gradient and degree of damage of PSII (Yuan et al., 2013). In our study, $Y(ND)$ in Zhangza 5 increased at the fluroxypyr concentrations of $\leq 1 \text{ L ai ha}^{-1}$.

To further understand the mechanism of fluroxypyr toxicity about Zhangza 5, we analyzed the effect of fluroxypyr on endogenous hormones. Herbicides induced changes in endogenous hormones and regulated stomatal behavior. Zhou et al. (2014) reported that the stomatal behavior of plant leaves is related not only to their content of endogenous hormones, but also to the balance of various hormones. Wang, Zhou & Zhou (1994) reported that stomatal closure and transpiration reduction are affected by ABA, and also result from the combined action of ABA and ZR. In the present study, the IAA and ABA contents in the plant leaves were significantly increased; however, the GA and ZR contents significantly decreased. In our study, G_s values showed a progressive decrease with the increase in fluroxypyr concentrations, while ABA content gradually accumulated with the increase in fluroxypyr concentrations, implying that ABA inhibited photosynthesis by decreasing stomatal conductance. In addition to stomatal regulation, ABA and ZR also directly influenced

photosynthesis. ABA reduced the electric potential of the chloroplast cell membrane, thereby reducing photosynthetic electron transport, whereas ZR could increase the Rubisco activity and promote photosynthetic electron transport.

High efficiency and safety are the main objectives of herbicide application. Eleven simplified indicators were screened by Fisher discriminant analysis, and principal component analysis was used to comprehensively evaluate the growth parameters, peroxidation characteristics, photosynthetic characteristics and endogenous hormones of foxtail millet at different fluroxypyr dosages. The model was set up as follows: $F = 0.592Z_1 + 0.345Z_2$. The cumulative contribution rate of the first two principal components reached 93.72%. The first principal component explained 59.23% of the variance including photosynthetic characteristics and endogenous hormones of foxtail millet. The second principal component accounted for 34.49% of the variance and had high loadings for growth parameters. Consequently, these two principal components were selected to represent the comprehensive effect of fluroxypyr on foxtail millet.

CONCLUSIONS

The effect of fluroxypyr on foxtail millet is complex and involves combination of several factors. The application of 1 L ai ha⁻¹ fluroxypyr exerted minimal effects on growth parameters, oxidase activity, photosynthetic activity, and endogenous hormones, indicating its efficient and safe benefits in foxtail millet application.

ACKNOWLEDGMENTS

We are gratefully acknowledgment help from Professor Yuguo Wang, Shanxi Agricultural University, for suggestion on the manuscript. Thanks are also due to three anonymous reviewers and editor for their thoughtful and valuable comments and suggestions, which helped in improving the manuscript.

REFERENCE

- [1]Rubin B. 1996. Herbicide-resistant weeds – the inevitable phenomenon: mechanisms, distribution and significance. *Z. Pflkrankh. Pflschutz* XV 17–32
- [2]Chen J, Shiyab S, Han FX, Monts DL, Waggoner CA, Yang ZM, Su Y. 2009. Bioaccumulation and physiological effects of mercury in *Pteris vittata* and *Nephrolepis exaltata*. *Ecotoxicology* 18:110–121
- [3]Christof K, Ulrich S. 2008. Complementary PS II quantum yields calculated from simple fluorescence parameters measured by PAM fluorometry and the saturation pulse method. *PAM Apply Notes* 1:27–35
- [4]Deng CN, Zhang DY, Pan XL, Chang FQ, Wang SZ. 2013. Toxic effects of mercury on PSI and PSII activities, membrane potential and transthylakoid proton gradient in *Microsorium pteropus*. *Journal of Photochemistry and Photobiology B: Biology* 127:1–7
- [5]Dong BD, Liu MY, Jiang JW, Shi CH, Wang XM, Qiao YZ, Liu YY, Zhao ZH, Li DX, Si FY. 2014. Growth, grain yield, and water use efficiency of rain-fed spring hybrid millet (*Setaria italica*) in plastic-mulched and unmulched fields. *Agricultural Water Management* 143:93–101
- [6]Elstner EF, Heupel A. 1976. Inhibition of nitrite formation from hydroxylammonium chloride: A simple assay for superoxide dismutase. *Analytical Biochemistry* 70:616–620
- [7]Grossmann K. 2010. Auxin herbicide: current status of mechanism and mode of action. *Pest Management Science* 66:113–120
- [8]Guo MJ, Wang YG, Dong SQ, Wen YY, Song XE, Guo PY. 2018. Photochemical changes and oxidative damage in four foxtail millet varieties following exposure to sethoxydim. *Photosynthetica* 56:820–831
- [9]Guo LW, Jing C, Ling T, Hong Y. 2010. Fluroxypyr triggers oxidative damage by producing superoxide and hydrogen peroxide in rice (*Oryza sativa*). *Ecotoxicology* 19:124–132

- 379 [10]Thiel H, Varrelmann M. 2014. Identification of a new PSII target site *psbA* muta-tion leading to D1 amino
380 acid Leu218 Val exchange in the *Chenopodiumalbum* D1 protein and comparison to cross-resistance profiles
381 of known modifications at positions 251 and 264. *Pest Management Science* 70:278–285
- 382 [11]Hellou J, Leonard J, Cook A, Doe K, Dunphy K, Jackman P, Tremblay L, Flemming JM. 2009.
383 Comparison of the partitioning of pesticides relative to the survival and behaviour of exposed amphipods.
384 *Ecotoxicology* 18:27–33
- 385 [12]Havaux M, Strasser RJ, Greppin H. 1991. A theoretical and experimental analysis of the qP and qN
386 coefficients of chlorophyll fluorescence quenching and their relation to photochemical and nonphotochemical
387 events. *Photosynthesis Research* 27:41–55
- 388 [13]Halliwell B, Foyer CH. 1978. Properties and physiological function of a glutathione reductase purified
389 from spinachleaves by affinity chromatography. *Planta* 139: 9–17
- 390 [14]Kehrer PP. 1993. Free radicals as mediators of tissue injury and disease. *Critical Reviews in Toxicology*
391 23:21–48
- 392 [15]Khan SM, Kour G. 2007. Subacute oral toxicity of chlorpyrifos and protective effect of green tea extract.
393 *Pest Biochemistry and Physiology* 89:118–123
- 394 [16]Klughammer C, Schreiber U. 2008. Saturation Pulse method for assessment of energy conversion in PS I.
395 *PAM Apply Notes* 1:11-14
- 396 [17]Lichtenthaler HK. 1987. Chlorophylls and carotenoids: pigments of photosynthetic biomembranes.
397 *Methods in Enzymology* 148:350-382
- 398 [18] Liu LC. 2014. Study 20% fluroxypyr control broadleaf weeds in maize field. *Modernizing Agriculture*
399 417:4-5(in chinese)

- 400 [19]Vila-Aiub MM, Goh SS, Gaines TA, Han HP, Busi R, Yu Q, Powles SB. 2014. No fitnesscost of
401 glyphosate resistance endowed by massive EPSPS gene amplification in *Amaranthus palmeri*. *Planta*
402 239:793–801
- 403 [20]Matzrafi M, Gadri Y, Frenkel E, Rubin B, Peleg Z. 2014. Evolution of herbicide resistance mechanisms in
404 grass weeds. *Plant Science* 229:43–52
- 405 [21]Nakano Y, Asada K. 1981. Hydrogen peroxide is scavenged by ascorbate specific peroxidase in spinach
406 chloroplasts. *Plant and Cell Physiology* 22:867–880
- 407 [22]Tranel PJ, Wright TR, Heap I. 2014. ALS Mutations from Herbicide-resistant Weeds.
408 <http://www.weedscience.com>
- 409 [23]Pfündel E, Klughammer C, Schreiber U. 2008. Monitoring the effects of reduced PS II antenna size on
410 quantum yields of photosystems I and II using the Dual-PAM-100 measuring system. *PAM Apply Notes* 1:21–
411 24
- 412 [24]Qian HF, Tsuji T, Endo T, Sato F. 2014. The PGR5 and NDH pathways in photosynthetic cyclic electron
413 transfer respond differently to sub-lethal treatment with photosystem-interfering herbicides. *Journal of*
414 *Agricultural and Food Chemistry* 62:4083–4089
- 415 [25]Sammons RD, Gaines TA. 2014. Glyphosate resistance: state of knowledge. *Pest Management Science*
416 70:1367–1377
- 417 [26]Scheller HV, Haldrup A. 2005. Photoinhibition of photosystem I. *Planta* 221:5–8
- 418 [27]Kaundun SS. 2014. Resistance to acetyl-CoA carboxylase-inhibiting herbicides. *Pest Management Science*
419 70:1405–1417
- 420 [28]Gaines TA, Zhang W, Wang D, Bukun B, Chisholm ST, Shaner DL, Nissen SJ, Patzoldt WL, Tranel PJ,

421 Culpepper AS, Grey TL, Webster TM, Vencill WK, Sammons RD, Jiang J, Preston C, Leach JE, Westra P.
 422 2010. Gene amplification confers glyphosate resistance in *Amaranthus palmeri*. *Proceeding of the National*
 423 *Academy of Science of the USA* 107:1029–1034

424 [29]Tian BH, Wang JG. 2010. Study on selection of suitable herbicides for hybrid millet. *Journal of Hebei*
 425 *Agricultural Sciences* 14:46–47 (in Chinese)

426 [30]Wang YY, Zhou R, Zhou X. 1994. Endogenous levels of ABA and cytokinins and their relation to
 427 stomatal behavior in dayflower (*Commelina communis* L.). *Journal of Plant Physiology* 144:45–48

428 [31]Yuan XY, Guo PY, Qi X. Ning N, Wang H, Wang HF, Wang X, Yang YJ. 2013. Safety of herbicide
 429 Sigma Broad on *Radix Isatidis* (*Isatis indigotica* Fort.) seedlings and their photosynthetic physiological
 430 responses. *Pesticide Biochemistry and Physiology* 106:45–50

431 [32]Zhang GY, Liu X, Quan ZW, Cheng SF, Xu X, Pan SK, Xie M, Zeng P, Yue Z, Wang WL, Tao Y, Bian C,
 432 Han CL, Xia QJ, Peng XH, Cao R, Yang XH, Zhan DL, Hu JC, Zhang YX, Li HN, Li H, Li N, Wang JY,
 433 Wang CC, Wang RY, Guo T, Cai YJ, Liu CZ, Xiang HT, Shi QX, Huang P, Chen QC, Li YR, Wang J, Zhao
 434 ZH, Wang J. 2012. Genome sequence of foxtail millet (*Setaria italica*) provides insights into grass evolution
 435 and biofuel potential. *Nature Biotechnology* 30:549-556

436 [33]Zhou HZ, Liu HX, Bo KY, Jia HY, Lv P. 2012. Study on prediction model of millet yield loss caused by
 437 weeds in summer season millet field. *Journal of Agricultural* 2:12–15 (in Chinese)

438 [34]Zhou YF, Wang DQ, Liu ZB, Wang N, Wang YT, Li FX, Xu WJ, Huang RD. 2014. Effects of Drought
 439 Stress on Photosynthetic Characteristics and Endogenous Hormone ABA and CTK Contents in Green-Stayed
 440 Sorghum. *Scientia Agricultura Sinica* 47:655–663 (in chinese)

Figure 1

Figure 1. Effect of fluroxypyr on superoxide, peroxidase, catalase, ascorbate peroxidase, and glutathione reductase activities of foxtail millet.

SOD, POD, CAT, APX and GR represent superoxide, peroxidase, catalase, ascorbate peroxidase, and glutathione reductase activities, respectively.

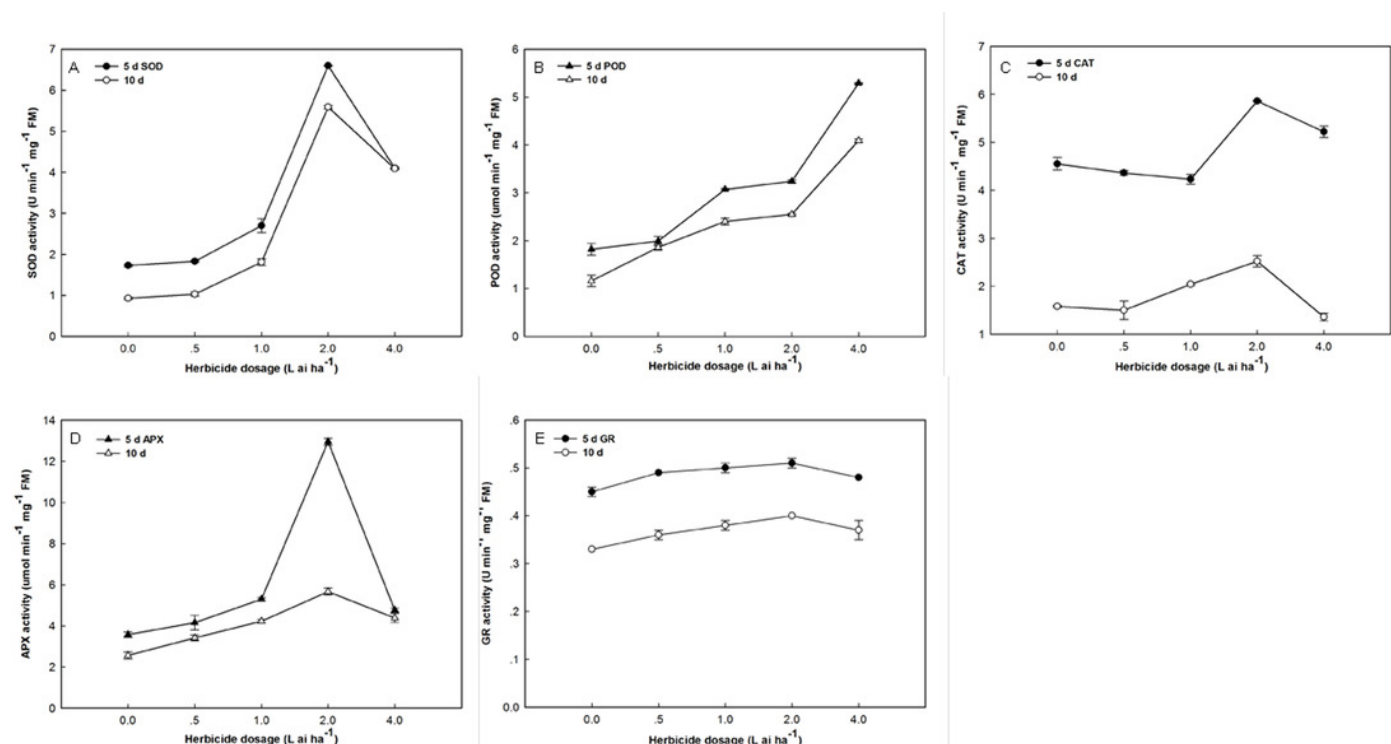


Figure 2

Figure 2. Effect of fluroxypyr on chlorophyll fluorescence and P_{700} parameters of foxtail millet.

F_v/F_m – maximum quantum yield of PS; $Y(II)$ – PSII effective quantum yield; $ETR(II)$ – PSII electron transport rate. $Y(NO)$ – quantum yield of nonregulated energy dissipation in PSII; $Y(NPQ)$ – quantum yield of regulated energy dissipation in PSII. P_m – maximal P_{700} change; $Y(I)$ – photochemical quantum yield of PSI; $ETR(I)$ – PSI electron transport rate; $Y(NA)$ – quantum yield of nonphotochemical energy dissipation due to acceptor-side limitation in PSI; $Y(ND)$ – quantum yield of nonphotochemical energy dissipation due to donor-side limitation in PSI.

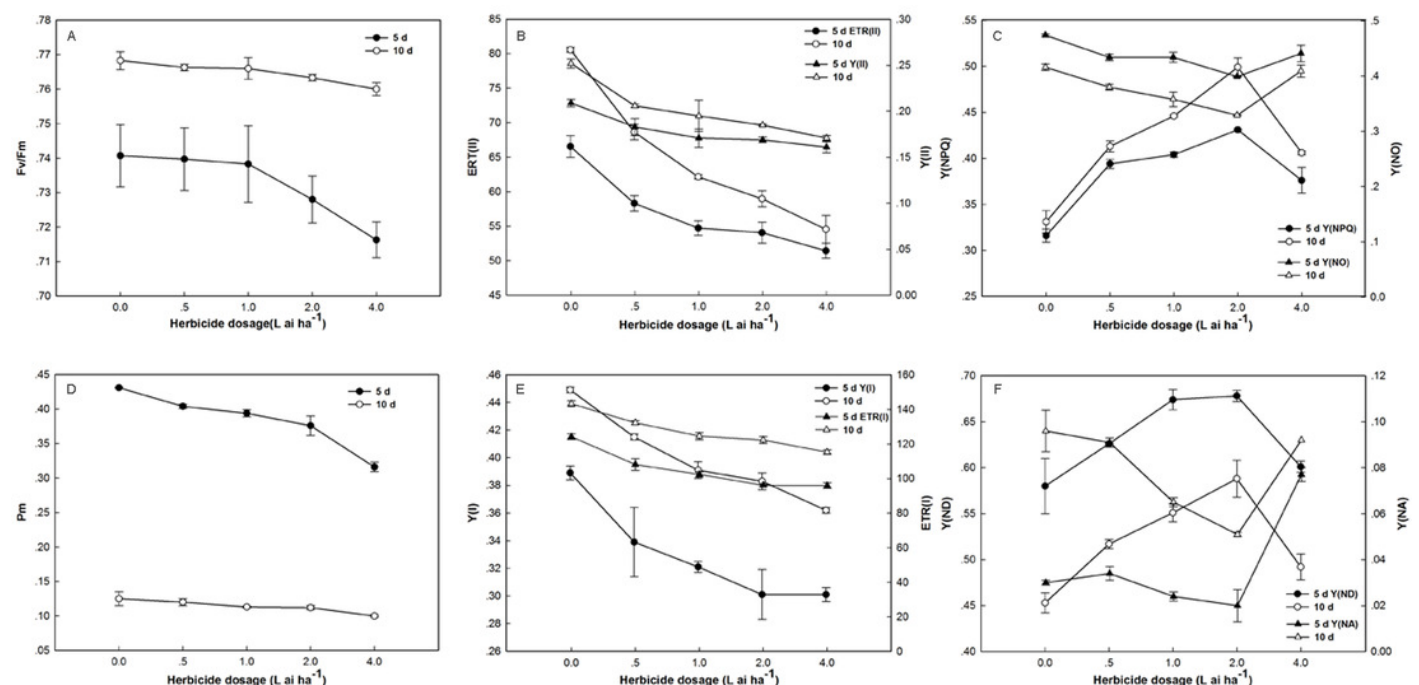


Figure 3

Figure 3. Effect of fluroxypyr on endogenous hormones of foxtail millet.

IAA, GA, ABA and ZR represent auxin, gibberellin, zeatin, abscisic acid, respectively.

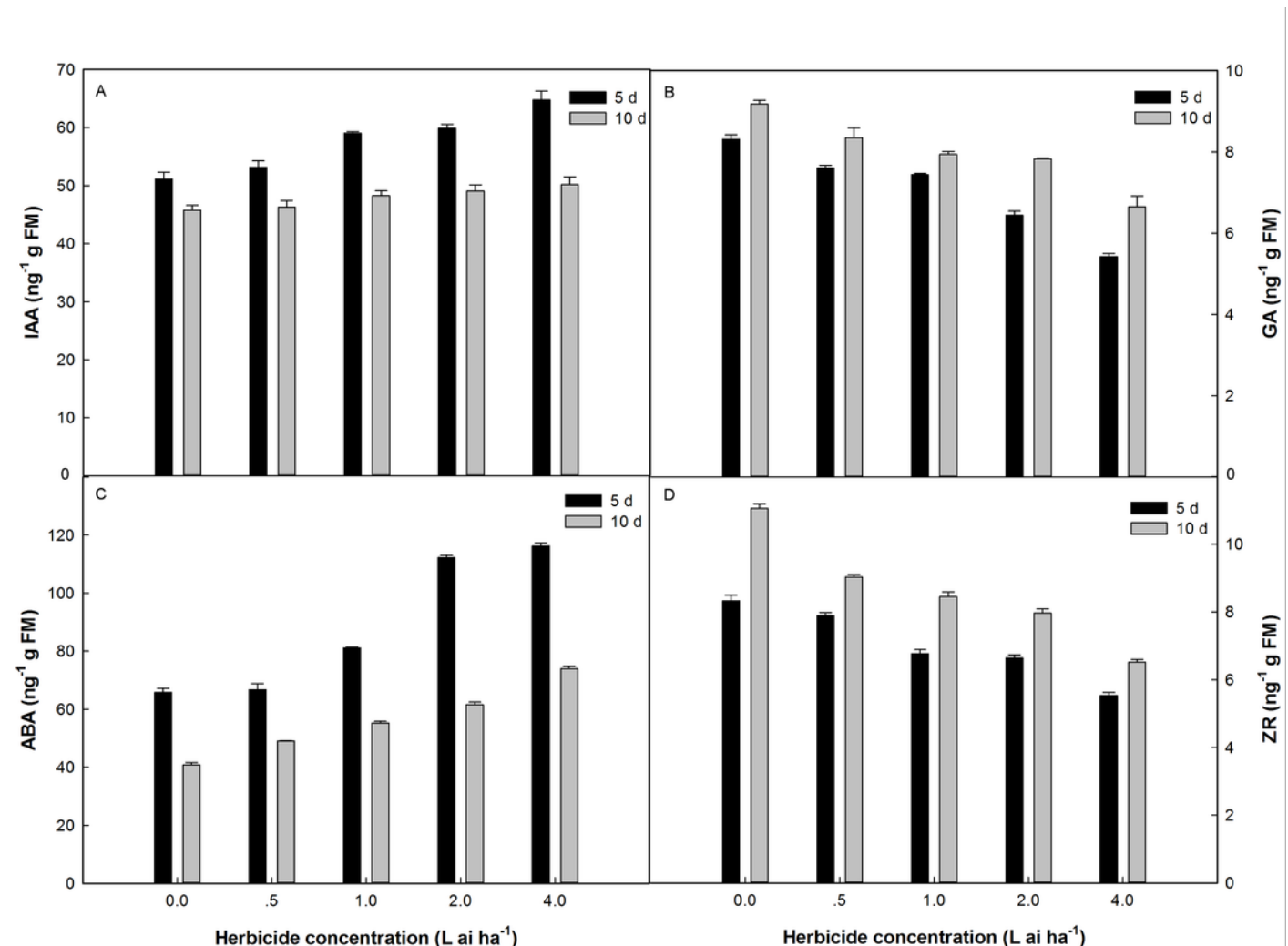


Figure 4

Figure 4. PCA score plot, the percentages of PC1 and PC2 representing the total variances of samples.

((1)-(3)) represent fluroxypyr dosage 4.0 L ai ha⁻¹, ((4)-(6)) represent fluroxypyr dosage 2.0 L ai ha⁻¹, ((7)-(9)) represent 0.5 L ai ha⁻¹, ((10)-(12)) represent fluroxypyr dosage 1.0 L ai ha⁻⁴, and ((13)-(14)) represent fluroxypyr dosage 0 L ai ha⁻¹, respectively.

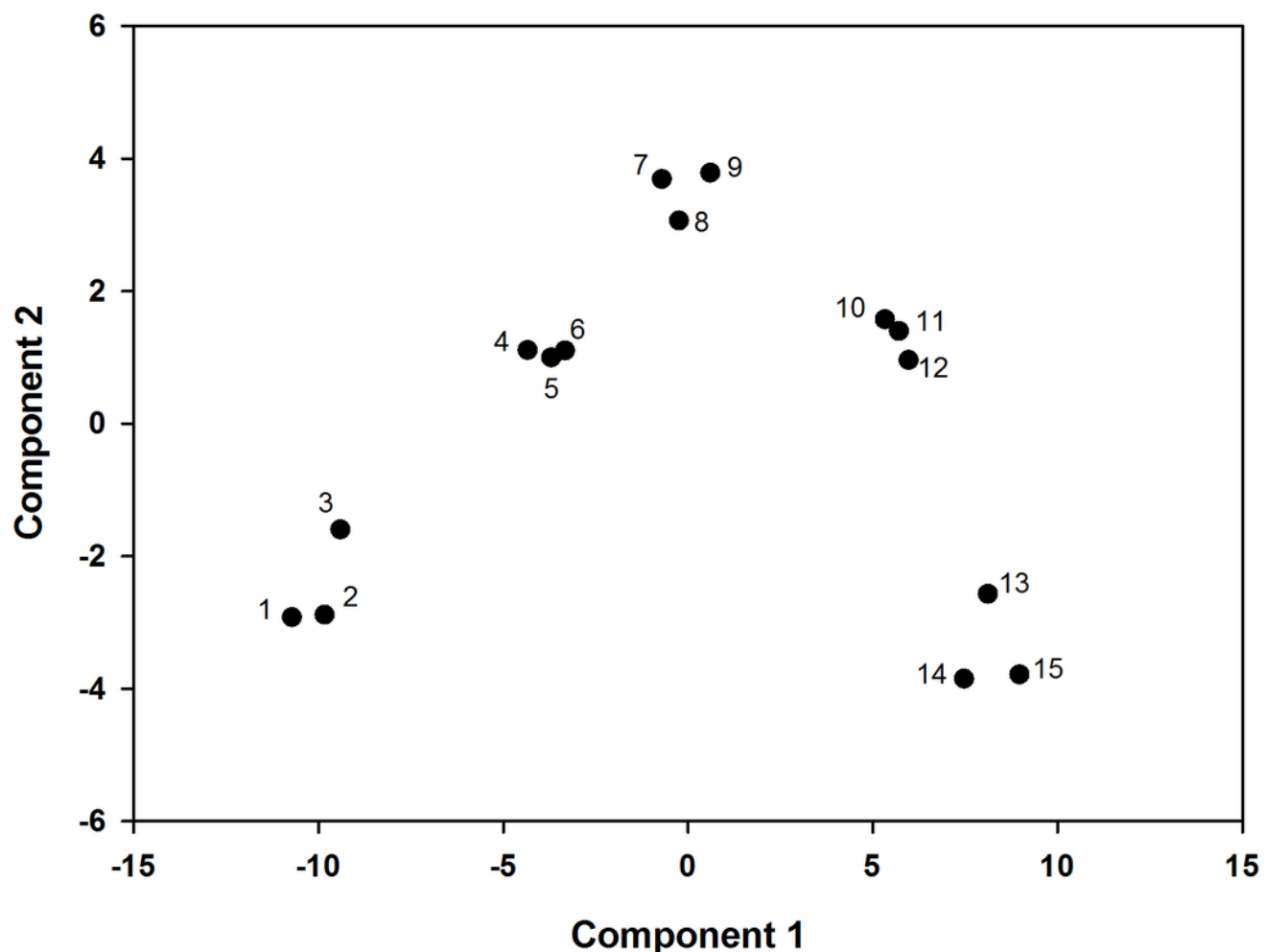


Table 1(on next page)

Table 1 Effect of fluroxypyr application on growth parameters in foxtail millet

Different letters in the same column indicate a significantly difference at the $P<0.05$ level by Duncan's new multiple range test.

Table 1 Effect of fluroxypyr application on growth parameters in foxtail millet

Herbicide dosage (L ai ha ⁻¹)	Plant height (cm)		Leaf area (cm ²)	
	5 Day	10 Day	5 Day	10 Day
0	26.05±0.23c	30.50±0.34cd	8.00±0.48b	12.10±0.15b
0.5	29.95±0.46b	33.60±0.57ab	9.71±0.07b	12.50±0.18b
1	32.50±0.02a	34.35±0.23a	13.94±0.43a	15.49±0.32a
2	28.60±1.41b	32.25±0.95bc	8.70±0.69b	12.18±0.36b
4	23.60±1.21d	30.10±0.02d	7.78±1.77b	10.75±0.33c

Different letters in the same column indicate a significantly difference at the $P<0.05$ level by Duncan's new multiple range test.

Table 2 (on next page)

Table 2 Effect of fluroxypyr application on stress parameters in foxtail millet

Different letters in the same column indicate a significant difference at the $P < 0.05$ level by Duncan's new multiple range test.

FM, fresh mass.

1

Table 2 Effect of fluroxypyr application on stress parameters in foxtail millet

Herbicide dosage (L ai ha ⁻¹)	H ₂ O ₂ content (umol g ⁻¹ FM)		O ₂ ⁻ generating rate (nmol g ⁻¹ min ⁻¹ FM)	
	5 Day	10 Day	5 Day	10 Day
0	40.70±0.02c	15.53±0.05e	164.18±1.09d	153.06±0.41c
0.5	40.83±0.02c	23.69±0.03d	167.26±0.34c	159.45±0.95b
1	41.16±0.03c	31.40±0.05c	168.20±0.54c	160.87±0.95b
2	42.96±0.01b	36.40±0.06b	177.19±0.85b	162.05±0.54b
4	51.30±0.03a	39.06±0.07a	193.28±0.41a	166.07±1.63a

2 Different letters in the same column indicate a significantly difference at the $P<0.05$ level by Duncan's new
 3 multiple range test.

4 FM, fresh mass.

Table 3 (on next page)

Table 3 Effect of fluroxypyr application on photosynthetic parameter and pigments in leaves of foxtail millet

Different letters in the same column indicate a significantly difference at the $P<0.05$ level by Duncan's new multiple range test. P_N , E , G_s and Chl represent photosynthetic rate, Transpiration rate, stomatal conductance, chlorophyll content, respectively.

Table 3 Effect of fluroxypyr application on photosynthetic parameter and pigments in leaves of foxtail millet

Herbicide dosage (L ai ha ⁻¹)	P_N [umol(CO ₂)m ⁻² s ⁻¹]		E [umol(H ₂ O ₂)m ⁻² s ⁻¹]		G_s [umol(CO ₂)m ⁻²]		Chl (mg g ⁻¹)	
	5 Day	10 Day	5 Day	10 Day	5 Day	10 Day	5 Day	10 Day
0	16.86±0.31a	26.56±0.14a	2.57±0.01a	4.76±0.09a	67.53±0.18a	120.99±2.76 a	9.57±1.13a	14.24±0.75 a
0.5	14.81±0.52b	23.81±0.73 b	2.17±0.06a b	4.31±0.02 b	61.81±2.09b	108.81±0.95 b	9.26±0.03a	13.82±0.24 a
1	12.86±0.48c	21.57±0.91 b	1.99±0.32b	4.04±0.01c	65.14±0.79a b	98.25±2.63c	8.33±0.50a b	13.55±0.09 a
2	11.88±0.47c d	22.27±1.13 b	1.72±0.09b c	3.85±0.10c	51.67±1.93c	91.68±4.74c	7.17±0.07b c	11.75±0.24 b
4	11.28±0.47d	16.95±0.36c	1.24±0.04c	3.16±0.03 d	50.03±1.63c	74.71±2.55d	5.83±0.21c	10.92±0.42 b

Different letters in the same column indicate a significantly difference at the $P<0.05$ level by Duncan's new multiple range test.

P_N , E , G_s and Chl represent photosynthetic rate, Transpiration rate, stomatal conductance, chlorophyll content, respectively.

Table 4(on next page)

Table 4 Component matrix and variance explained by principal component

1

Table 4 Component matrix and variance explained by principal component

Traits	Component weight	
	Component 1	Component 2
Plant height	0.189	0.975
Leaf area	0.146	0.888
SOD activity	0.175	0.965
POD activity	-0.926	-0.245
GR activity	-0.702	0.640
Y(II)	0.963	-0.233
Y(NPQ)	-0.652	0.653
P _m	0.944	0.255
ETR(I)	0.978	-0.206
GA	0.975	0.184
ABA	-0.963	-0.178
Eigenvalue	6.515	3.794
Cumulative contribution (%)	59.230	93.722

2

Table 5(on next page)

Table 5 Principal score and general score of comprehensive evaluation

1

Table 5 Principal score and general score of comprehensive evaluation

Treatment	Prin1 score	Prin2 score	Composite score F
0.5	0.083	2.585	0.941
1	2.998	0.672	2.007
2	-4.242	0.638	-2.291
4	-7.850	-2.110	-5.375

2